

Wave-Driven Mean Tropical Upwelling in the Lower Stratosphere

R. K. SCOTT

Laboratoire d'Aérodynamique, Observatoire Midi Pyrénées, Toulouse, France

(Manuscript received 27 June 2001, in final form 25 March 2002)

ABSTRACT

The mean meridional circulation induced by zonal momentum forcing is considered in the context of (i) a wave-mean model, in which the momentum forcing arises naturally from the explicit representation of the stratospheric wave response to lower boundary forcing, and (ii) a zonally symmetric model, in which the momentum forcing is prescribed externally. Wave forcing is confined to one hemisphere, as a simple representation of the difference between the Northern and Southern Hemispheres. The main focus of the paper is on how the upwelling branch of the circulation in the Tropics depends on nonlinearity, model diffusion, and the transient effects of the seasonal cycle. Significant tropical upwelling can occur in the steady state if the zonal momentum force extends into the subtropics, provided the forcing is strong enough to redistribute angular momentum throughout the Tropics. The circulation in these strongly forced cases depends nonlinearly on the forcing amplitude. If the forcing is weak, so that the dynamics are approximately linear, significant tropical upwelling can occur in the steady state if (i) the radiative equilibrium temperature is such that angular momentum contours tilt poleward and upward, as at the winter solstice, or (ii) the model diffusion is large. In seasonally varying cases, weak subtropical forcing can also induce a time average tropical upwelling through the interaction of the transient angular momentum distribution and the transient forcing. When the forcing is strong, the effect of the seasonal cycle leads to an increase in the tropical upwelling beyond that of the steady-state response.

1. Introduction

Crucial to our understanding of the chemical and radiative properties of the middle atmosphere is an understanding of the mean meridional circulation and its dynamical and radiative causes. By mean meridional circulation we mean a zonally averaged, long-term, systematic motion of air parcels that, in particular, averages over the more rapid, small-scale wave motions present throughout the atmosphere. This circulation plays an important role in carrying chemical species away from source regions and influencing the distribution of chemically active and radiatively important species (e.g., ozone). An example is the transport from the troposphere into the stratosphere of chemical species ultimately responsible for significant stratospheric ozone depletion in the Southern Hemisphere (SH). The transport and redistribution within the stratosphere of ozone itself also plays a fundamental role in the heating of the stratosphere. A recent series of anomalously cold Northern Hemisphere (NH) stratospheric winters, and the consequent implications for ozone chemistry, underline the importance of the radiative properties of the stratosphere. Finally, the meridional circulation itself also cre-

ates significant departures from local thermodynamic equilibrium, for example, near the tropical tropopause and in the polar winter stratosphere. [For a general overview, see, e.g., WMO (1985), Andrews et al. (1987), and a recent review in WMO (1999).]

Because of the angular momentum structure of the atmosphere, which is dominated by the contribution from the earth's axial rotation, a mean meridional velocity at a particular extratropical location cannot persist without a systematic zonal mean force acting at the same location. This force is required for parcels of air to cross the nearly vertical surfaces of constant angular momentum. Such effects have been recognized since the works of Dickinson (1968, 1969), and have been discussed more recently in Held and Hou (1980), and Haynes et al. (1991). The latter derived an expression for the zonally symmetric, steady-state vertical velocity at a given location, completely in terms of the zonal momentum force above that location, integrating upward along a path of constant angular momentum. This expression [their Eq. (2.6)] makes explicit the concept of the "downward control" by a given distribution of zonal momentum forcing. In the real atmosphere, such a forcing arises from breaking planetary and gravity waves in the stratosphere and mesosphere. Holton (1990) and Rosenlof and Holton (1993) applied the downward control concept to observed eddy momentum and heat fluxes in

Corresponding author address: Dr. Richard K. Scott, Dept. of Applied Physics and Applied Mathematics, Columbia University, 200 Seeley W. Mudd Building, 500 W. 120th Street, New York, NY 10027.
E-mail: scott@appmath.columbia.edu

the stratosphere to deduce mass fluxes across the extratropical lower stratosphere and, by mass continuity, the upward mass flux in the Tropics.

The steady-state downward control expression can be extended to the case of a periodic forcing and response, allowing a representation of the annual quasiperiodicity of the atmosphere. Denoting the time average of a quantity q by $\langle q \rangle = T^{-1} \int_0^T q dt$ and the departure as $q' = q - \langle q \rangle$, and following the analysis of Haynes et al. (1991), the transformed Eulerian mean zonal momentum equation yields the following expression for the residual vertical velocity w^* :

$$\langle w^* \rangle = \frac{1}{\rho_0 a \cos \phi} \times \frac{\partial}{\partial \phi} \left\{ \int_z^\infty \left[\frac{\rho_0 a^2 \langle F \rangle \cos^2 \phi - \langle J \rangle}{\langle m_\phi \rangle} \right]_{\phi=\phi(z')} dz' \right\}. \quad (1)$$

Here, (ϕ, z) are log-pressure coordinates, $\rho_0(z)$ is density, F is the prescribed zonal force per unit mass, $J = \partial(\psi', m')/\partial(\phi, z)$ is the Jacobian determinant of the time-varying components of the streamfunction ψ and angular momentum m , and the integral is along a path $\phi(z)$ of constant m . Below, we will use (1) to determine the extent to which the interaction of the transient terms J , arising from an imposed seasonal cycle in thermal and momentum forcing, influences the residual circulation, with particular emphasis on the low-latitude upwelling circulation.

Despite a good understanding of the mechanisms involved in driving the observed mean meridional circulation in the extratropics, we still do not have a clear idea of those involved in low latitudes, where surfaces of constant angular momentum deviate significantly from the vertical, and where the dynamical link between the zonal mean velocity and temperature fields is weaker. In particular, there is still no complete explanation of the nonzero, time-averaged upward motion observed throughout low latitudes in the lower stratosphere. Yulaeva et al. (1994) derived the diabatic vertical ascent in the Tropics and found a seasonal cycle with a maximum in NH winter, consistent with the stronger wave activity in the NH stratosphere. However, even in the annual mean, the net ascent in the Tropics is still positive, which, according to (1), with a realistic distribution of m and neglecting transient terms appearing in J , cannot be explained by extratropical wave forcing alone.

Recently, Plumb and Eluszkiewicz (1999; hereafter PE99) considered the extent to which the downward control principle could account for the time mean diabatic ascent rates observed in the Tropics. In the context of zonally symmetric model simulations, they found that very small zonal forces arising from artificial viscosity (required for model stability) were ultimately responsible for driving the low-latitude response in the lower

stratosphere. Because of the vanishingly small angular momentum gradients in the Tropics, such small low-latitude forces can result in a significant tropical upwelling response, as can be seen from (1). Although the model viscosity in their study is artificial, the general point remains the same: that very small zonal forces, arising in the atmosphere, for example, from the breaking of equatorial waves or other weak wave breaking effects, are able to drive a significant circulation in low latitudes.

In the present paper, we examine the dependence of the tropical upwelling on mechanical forcing, together with the effects of low-latitude diffusive-type forces of the sort considered by PE99, nonlinearity, and the transient interaction of the seasonal cycle with the forcing. The latter is represented by the term J in (1), which is nonzero if there is time correlation between the transience of the angular momentum distribution (forced by the seasonal cycle in the radiative basic state) and the unsteady meridional circulation response to time varying mechanical forcing. To investigate these effects, we first use a model in which the waves are explicitly resolved, the zonal momentum force taking the form of the Eliassen–Palm (EP) flux divergence, arising self-consistently from wave dissipation in the model. Perpetual winter and seasonally evolving basic states are both considered. Further calculations using a zonally symmetric model are later used to analyze in more detail some of the features seen in the wave model, and how these arise from diffusive, nonlinear, and transient effects.

The structure of the paper is as follows. Section 2 contains a brief description of the model. Section 3 considers the response to wave forcing in the zonally asymmetric model, using the amplitude of the lower boundary wave forcing as an external parameter, and considering the dependence of the meridional circulation response as this parameter is changed. The response depends on the details of the stratospheric wave evolution rather than showing a simple dependence on the wave forcing amplitude. Section 4 considers the response to prescribed zonal momentum forcing in the zonally symmetric model. First the forcing is prescribed to be the EP flux divergence obtained from the zonally asymmetric model simulations, and the response is verified to follow closely that of the zonally asymmetric model. Thereafter, the forcing is given a meridionally compact analytic structure, enabling a more detailed investigation of the response to forcing in particular latitude ranges. Again, both steady and seasonally varying radiative basic states are considered. In section 5, we discuss in more detail the results of the zonally symmetric simulations of section 4. It is shown how numerical diffusion and the transience associated with the seasonal cycle both play an important role in modifying the low-latitude circulation. Conclusions are presented in section 6.

2. Model description

The model used is a mechanistic primitive equation model in spherical geometry, and is used here in essentially the same configuration as that described in Scott and Haynes (2002), to which the reader is referred for more complete details. It was originally developed by Saravanan (1992). There are 31 vertical levels equally spaced in $\log p$, where p is the pressure, with the lowest model level near 11 km and the highest near 83 km. A spectral representation is used in the horizontal comprising $M = 32$ or $M = 64$ meridional modes, with further truncation in the zonal direction as follows. In section 3, waves are explicitly represented in the model by including the zonal mean and the first (wavenumber-one) zonal mode. This severe zonal truncation is deemed to adequately capture the most important features of the stratospheric response for present purposes (Haynes and McIntyre 1987). Scott and Haynes (2002) showed that the effect of adding further zonal wavenumbers in numerical simulations of a similar nature to those presented below was small. In section 4 there is no zonal structure at all and the model corresponds to a zonally symmetric atmosphere.

The model is forced radiatively by including Newtonian relaxation to a zonally symmetric radiative equilibrium potential temperature θ_R that may be either constant in time or time varying, the latter case providing an approximation to the annual cycle. The height–latitude distribution of θ_R is determined as that which is in thermal wind balance with a specified semirealistic distribution of zonal winds. In sections 3 and 4a, the time-varying distribution of θ_R is specified exactly as in Scott and Haynes (2002, section 3 therein), and the steady distribution of θ_R is set to the winter solstice of the time-varying distribution. The relaxation timescale is approximately 20 days throughout the stratosphere and there is a sponge layer above 50 km. In section 4b, a time-varying θ_R is used that is antisymmetric about the equator (to give an annually averaged θ_R in thermal wind balance with a resting atmosphere), the relaxation timescale is 20 days, and there is no sponge layer.

In the zonally asymmetric version of the model, waves are forced by applying a wave-one perturbation to the geopotential height at the lower boundary. The forcing is restricted to the NH only, with zero amplitude south of 30°N, and maximum amplitude h_0 at 60°N. This restriction of the forcing provides a crude model of the stronger forcing of planetary waves in the NH by orographic effects and land–sea temperature contrasts compared with that in the SH. The forcing amplitude h_0 is held constant throughout each simulation (after a smooth switch-on time of 10 days) and is treated as an external parameter. In the zonally symmetric version of the model, a prescribed body force $F(\phi, z, t)$ is applied to the zonal momentum equation in the stratosphere. Various forms of F will be considered, including steady and seasonally varying.

Finally, scale-selective horizontal diffusion and vertical diffusion are included for model stability. The former is included as a ∇^8 hyperdiffusion, with a value of four per day on the smallest wavenumber, and the latter has a value of 0.1 m s⁻², except in section 4b, when it is zero.

3. Zonally asymmetric model results

We first consider the diabatic circulation induced in the zonally asymmetric configuration of the model by wave dissipation and thermal forcing. The model is truncated in the zonal direction to include only the zonal mean and the first zonal wavenumber, and waves are forced by a wave-one perturbation in the lower boundary geopotential height field with amplitude h_0 . Here, h_0 is varied as an external parameter, taking incremental values between $h_0 = 200$ m and $h_0 = 300$ m.

We present two sets of experiments: one, W_{steady} , in which the radiative basic state is constant in time and corresponds to perpetual winter; the other, W_{seasonal} , in which the radiative basic state is time varying and corresponds to the seasonal cycle in solar heating. In each, we consider the vertical component of the diabatic circulation, defined by

$$w^d = \frac{\overline{Q}}{\theta_{0z}}, \quad (2)$$

where $Q = \alpha(\theta_R - \theta)$ is the diabatic heating in the model due to radiative relaxation at rate α to the radiative equilibrium potential temperature θ_R , and where $\theta_0(z)$ is a reference potential temperature profile. Overbars denote a zonal average. The diabatic circulation w^d is an approximation to the full transformed Eulerian mean (TEM) residual circulation w^* under the condition of small local potential temperature tendency $\partial\theta/\partial t$ and neglecting ageostrophic eddy heat transport, both reasonable in the lower stratosphere (see, e.g., Shine 1989).

a. Perpetual winter

Figure 1a shows the response w^d at 17-km altitude as a function of latitude to lower boundary wave forcing amplitudes $h_0 = 0, 240, 260, 270,$ and 290 m. Recall that the wave forcing is restricted to the NH only (and poleward of 30°N). In all cases there is downwelling in mid- and high latitudes, accompanied by upwelling in low latitudes, which extends considerably into the opposite hemisphere from that in which the waves are forced. An important feature of Fig. 1a is the dependence of w^d on the amplitude of the lower boundary wave forcing.

For $h_0 = 0$ m, w^d is almost indistinguishable from zero everywhere, and would indeed be identical to zero everywhere were it not for the model diffusion and artificial viscosity (∇^8 hyperdiffusion and vertical viscosity), which prevents the temperature from exactly

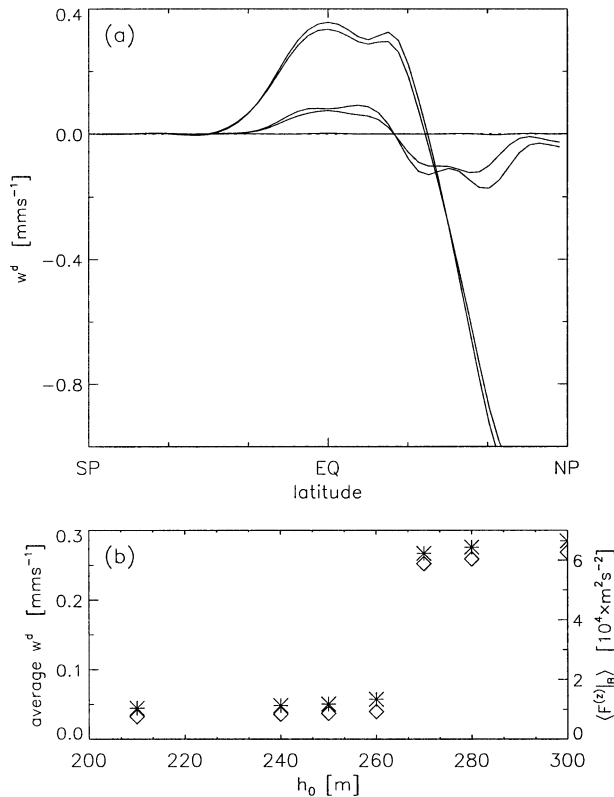


FIG. 1. Diabatic vertical velocity w^d at 17 km calculated by (2) and averaged over the last 100 days of 1000-day simulations, obtained with steady radiative basic state and lower boundary forcing amplitude h_0 . (a) $h_0 = 0$, $h_0 = 210$, $h_0 = 260$, $h_0 = 270$, $h_0 = 300$ in order of increasing magnitude of w^d . (b) w^d averaged over the latitude range $[-30^\circ, 30^\circ]$ for various forcing amplitudes (stars and left axis) together with the total upward EP flux through the lower boundary for the same time period and forcing amplitudes (diamonds and right axis).

following the radiative equilibrium potential temperature θ_R . This is because θ_R has been determined from thermal wind balance with a specified wind profile that is finite at the equator, and so $\partial\theta_R/\partial\phi$ must be zero at the equator. As noted by Dunkerton (1989), a nonzero $\partial\theta_R/\partial\phi$ at the equator is required for efficient thermal driving of a low-latitude circulation (see also PE99; Semeniuk and Shepherd 2001a,b). The present choice of θ_R therefore enables a partial isolation of the wave-driven circulation from the thermally driven circulation in low latitudes. In particular, note that the response w^d due to stratospheric thermal forcing alone, that is, that obtained with $h_0 = 0$, depends entirely on the viscosity, and that for small, physically reasonable values, the thermal response is at least an order of magnitude smaller than the wave-driven response obtained with physically reasonable values of wave forcing (the other solid curves in Fig. 1a). Note that while this approximation is appropriate in the lower stratosphere, the thermal response in the upper stratosphere is probably more important.

For forcing values between $h_0 = 0$ m and $h_0 = 260$ m the magnitude of w^d increases steadily with increasing forcing amplitude. However, between $h_0 = 260$ m and $h_0 = 270$ m there is a sudden increase to a significantly stronger response, as well as a shift in the latitudinal structure of the response. Beyond $h_0 = 270$ m the magnitude of w^d again increases gradually with further increase in forcing amplitude. Note that simple scaling considerations would suggest that the magnitude of w^d would be a quadratic function of h_0 .

The sudden change in w^d between $h_0 = 260$ m and $h_0 = 270$ m can be related to the meridionally averaged vertical component of the Eliassen–Palm flux at the lower boundary, $\langle F^{(z)}|_B \rangle^{\phi}$, given by

$$\begin{aligned} \langle F^{(z)}|_B \rangle^{\phi} &\equiv \frac{1}{2\pi a^2} \int_0^{\pi/2} F^{(z)} \cos\phi \, d\phi \Big|_{z=z_B} \\ &= -\frac{1}{2\pi a^2} \int_V \rho_0 F a \cos\phi \, dV = -\frac{1}{2\pi a^2} T, \end{aligned} \quad (3)$$

where $F = (1/\rho_0 a \cos\phi) \nabla \cdot \mathbf{F}$ is the force per unit mass, $\mathbf{F} = (F^{(\phi)}, F^{(z)})$ is the Eliassen–Palm flux [as defined by, e.g., Andrews et al. 1987, Eq. (3.5.3)], V denotes the domain of the model (i.e., the stratosphere), and T is the total torque produced by the waves on the zonal mean flow. The quantity F in the second line of (3) can be identified with the F in (1) and we therefore expect $\langle F^{(z)}|_B \rangle^{\phi}$ to be directly related to the magnitude of the response w^d . Figure 1b shows a strong correlation between $\langle F^{(z)}|_B \rangle^{\phi}$ and the tropically averaged w^d over a range of forcing amplitudes, even though the details of the response are ultimately governed not only by the magnitude of $\langle F^{(z)}|_B \rangle^{\phi}$ but also by the distribution of F within the stratosphere. The larger than expected increase in $\langle F^{(z)}|_B \rangle^{\phi}$ and hence in w^d from $h_0 = 260$ m and $h_0 = 270$ m arises because of two qualitatively distinct stratospheric equilibrium states that exist for the different forcing values (see Scott and Haynes 2000 for details).

The EP cross sections for representatives of the two states are shown in Fig. 2 and illustrate the different distributions of wave dissipation (as represented by the EP flux divergence). In both cases, the region where $\nabla \cdot \mathbf{F}$ is negative (i.e., where there is wave dissipation) is confined to north of the equator, and therefore (1) cannot explain the substantial upwelling all through the Tropics and into the opposite hemisphere [restricting attention to those regions where $\bar{m}_\phi \neq 0$ so that the integral in (1) is valid, e.g., south of around 5° – 10° S]. We will see in section 5 that the extension of the upwelling into the opposite hemisphere can be accounted for by considering the small zonal forces arising from artificial model diffusion, as described in PE99, together with the distortion of the angular momentum contours, in the case of Fig. 2 caused by the wave forcing itself.

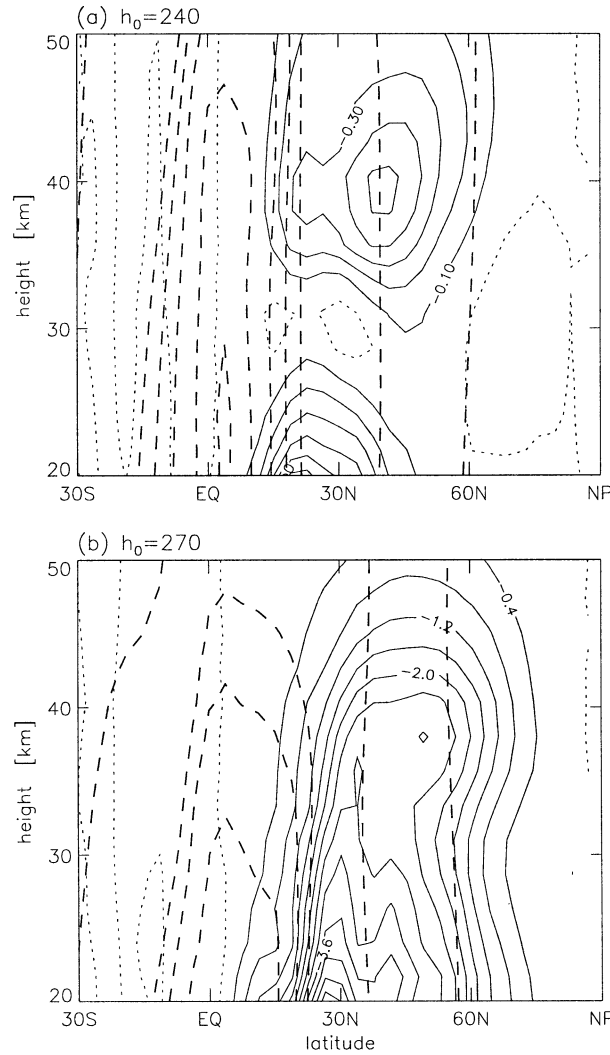


FIG. 2. EP flux convergence for two of the cases shown in Fig. 1: (a) for $h_0 = 240$ m and (b) for $h_0 = 270$ m. Solid lines denote negative values (divergence) and dotted lines denote positive values, in units of $2\pi a^3 \rho_e \times 10^{-7} \text{ m s}^{-2}$; note the different contour interval between the two plots. Also shown dashed are various contours of constant angular momentum (contour values not important).

b. Seasonally varying radiative basic state

In this section we consider the induced meridional circulation when a representation of the seasonal cycle in solar heating is included in the radiative equilibrium state. The form of the seasonal cycle is given by

$$\theta_R = r\theta_{RS} + (1 - r)\theta_{RW}, \quad (4)$$

$$r(t) = \frac{1}{2} \left(1 + \cos \frac{2\pi t}{365 \text{ days}} \right), \quad (5)$$

and is a sinusoidal superposition of summer and winter basic states θ_{RS} and θ_{RW} as defined in Scott and Haynes (2002, section 3). Because propagation of wave activity into the model domain from the lower boundary is re-

stricted to times when the zonal flow is westerly, the seasonal cycle in basic state also gives rise to a seasonal cycle in wave dissipation in the stratosphere.

First consider the response to radiative forcing alone. Under seasonally evolving conditions the potential temperature follows the radiative basic state with a time lag dependent on the relaxation rate, so the radiative forcing will be nonzero throughout the year. Figure 3a shows w^d as defined by (2) for this case ($h_0 = 0$). The seasonal cycle is clear in the extratropics, with downwelling in the autumn, when the vortex is warmer than the radiative basic state, and upwelling in the spring, when it is colder. In the Tropics, there is still a seasonal cycle but, again, since $\partial\theta_R/\partial\phi = 0$ at the equator, it is very weak, with values of w^d less than 0.01 mm s^{-1} throughout the range (15°S – 15°N). The weakness of the thermally driven circulation allows a clearer focus on the wave-driven circulation.

For nonzero lower boundary wave forcing the resulting wave dissipation in the stratosphere modifies the thermally driven circulation. For $h_0 = 240$ m there is a substantial increase in the low-latitude response (Fig. 3b), with maximum upwelling of 0.12 mm s^{-1} , and a corresponding increase in the NH winter downwelling. For $h_0 = 270$ m there is a still larger increase in the low-latitude response (Fig. 3c), with maximum equatorial upwelling in excess of 0.24 mm s^{-1} , and subtropical upwelling reaching 0.54 mm s^{-1} in NH spring. Note that for $h_0 = 270$, the model response (to steady wave forcing and annually periodic heating) exhibits an internal biennial oscillation of the type investigated in Scott and Haynes (1998), in which quiescent and disturbed winters alternate, and this signal is clearly visible in w^d . As in section 3a the difference in w^d between the disturbed and quiescent years is again correlated with the meridionally averaged upward component of the EP flux through the lower boundary.

The annually averaged w^d is shown in Fig. 4 for the forcing amplitudes $h_0 = 0, 210, 240,$ and 270 m. There is a marked increase in response between the $h_0 = 240$ and $h_0 = 270$ m cases, though less dramatic than for the steady case above. There is also a clear difference between the annually averaged w^d of the disturbed and quiescent years obtained with $h_0 = 270$ m (dotted lines). Note that the annually averaged w^d for $h_0 = 0$ is everywhere small and almost indistinguishable from zero in the Tropics.

4. Zonally symmetric model results

To help understand the nature of the wave-driven circulation, we consider the response of a zonally symmetric version of the model to a prescribed zonal momentum force, designed to represent the forcing that arises from wave dissipation in the zonally asymmetric model. The residual circulation (v^*, w^*) of the TEM formulation is now just the zonally symmetric circulation (v, w). For uniformity with section 3, we continue

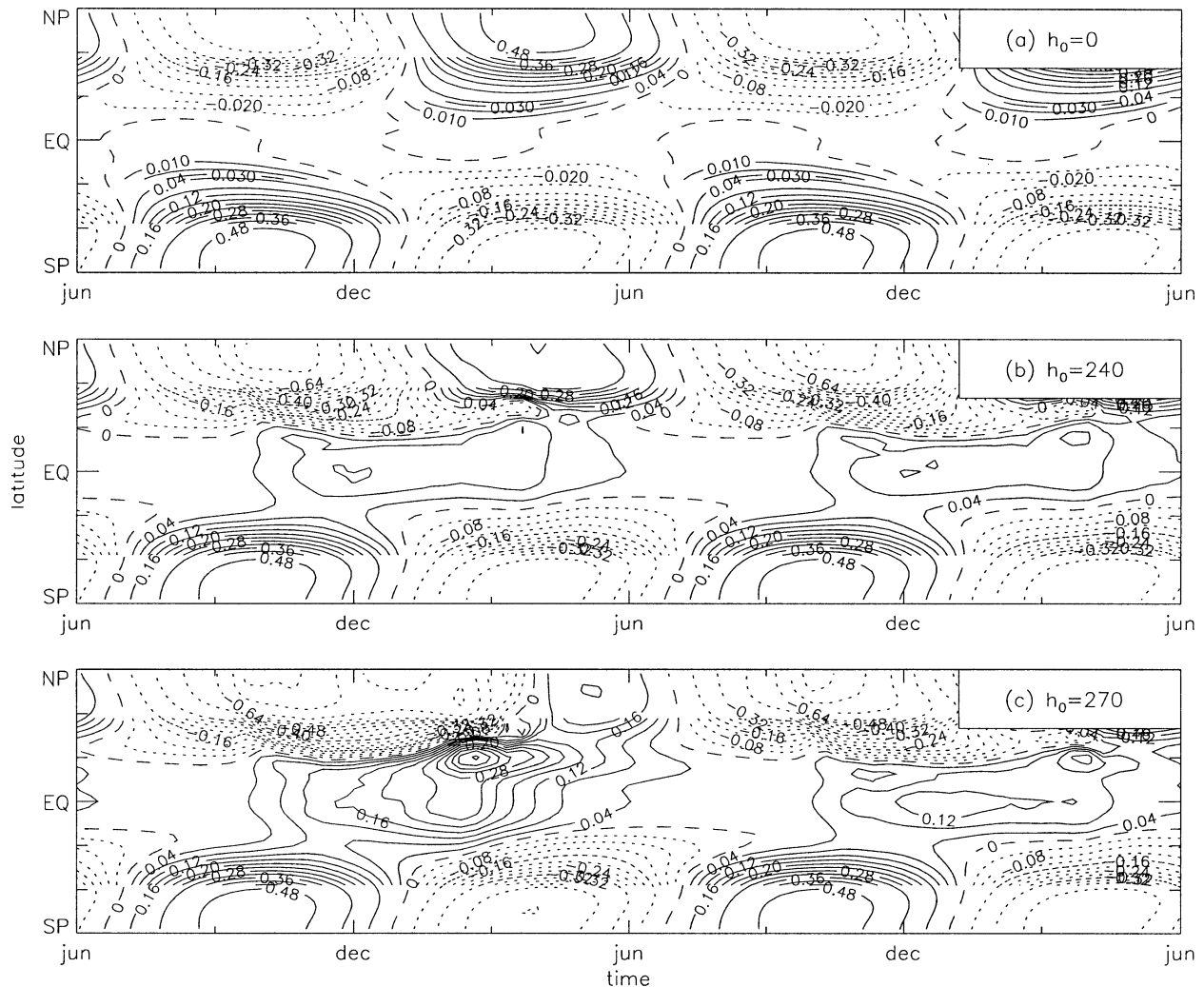


FIG. 3. Diabatic vertical velocity w^d at 17 km as a function of time and latitude, taken from the last 2 yr of 10-yr simulations with a seasonally varying radiative basic state, but constant lower boundary forcing amplitude h_0 : (a) for $h_0 = 0$, (b) for $h_0 = 240$ m, and (c) for $h_0 = 270$ m. The contour interval is 0.04 mm s^{-1} equatorward of $\pm 60^\circ$ and 0.16 mm s^{-1} poleward of $\pm 60^\circ$, except in (a), which has additional contours equatorward of $\pm 30^\circ$ at intervals of 0.01 mm s^{-1} .

to use the vertical component of the diabatic circulation w^d as our principal diagnostic. It has been verified that the difference between w and w^d is in general small in all of the following cases.

a. Zonal forcing derived from the asymmetric model

We first investigate the extent to which the meridional circulations produced in the wave-one model of the previous section can be reproduced in the zonally symmetric model using an applied zonal momentum force that is derived from the EP flux divergence of the wave-one model. Three sets of experiments are described. In the first, Z_{steady} , the radiative forcing is the same as that of the perpetual winter cases W_{steady} of section 2 above, and the prescribed zonal momentum force is the steady-state wave-induced zonal momentum force per unit mass

obtained with a lower boundary forcing amplitude of $h_0 = 240$ m, that is

$$F = \frac{1}{\rho_0 \cos \phi} \nabla \cdot \mathbf{F}, \quad (6)$$

where $\nabla \cdot \mathbf{F}$ is the EP flux divergence output from W_{steady} with $h_0 = 240$ m. In the second set, Z_{seasonal} , the radiative forcing, is the same as that of the seasonally varying cases, W_{seasonal} , of section 2, and the zonal momentum force is the seasonally varying wave-induced zonal momentum force per unit mass produced by W_{seasonal} with $h_0 = 240$ m. Finally, in the third set, Z_{mean} , both the radiative forcing and the zonal momentum force are constant in time and equal to the annual average of the values used in Z_{seasonal} . In all cases the zonal momentum force is smoothed in space and time to ensure a more stable response of the zonally symmetric model.

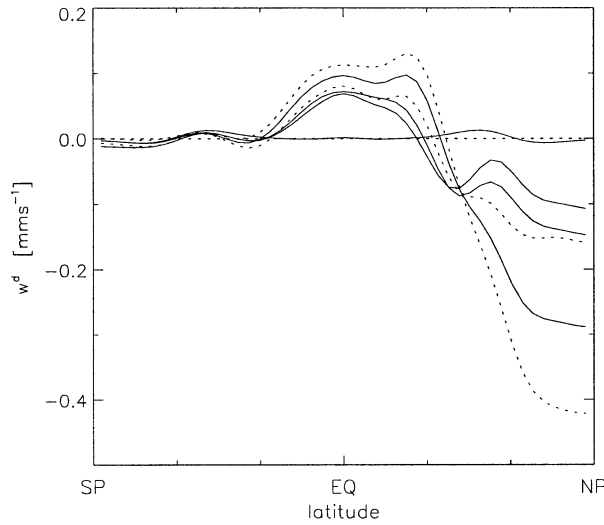


FIG. 4. Diabatic vertical velocity w^d at 17 km, as in Fig. 3, averaged over the 2-yr period. Solid lines show w^d for $h_0 = 0$ m, $h_0 = 210$ m, $h_0 = 240$ m, $h_0 = 270$ m in order of ascending magnitude; dotted lines show the consecutive annual averages of the case $h_0 = 270$ m.

The meridional distribution of F in the steady case Z_{steady} is shown in Fig. 2, and the time evolution and vertical structure of F in the seasonally varying case Z_{seasonal} is shown in Fig. 5. In each case, we see that F goes to zero at the equator. However, as already mentioned, small forces at low latitudes can still play an important role in driving a meridional circulation throughout the Tropics.

The results are summarized in Fig. 6, which shows the time average w^d at 17 km in the seasonally varying case. The solid and dashed lines represent w^d from the zonally symmetric and asymmetric models, respectively. The good agreement between the two responses is also present in the steady case (not shown). The good

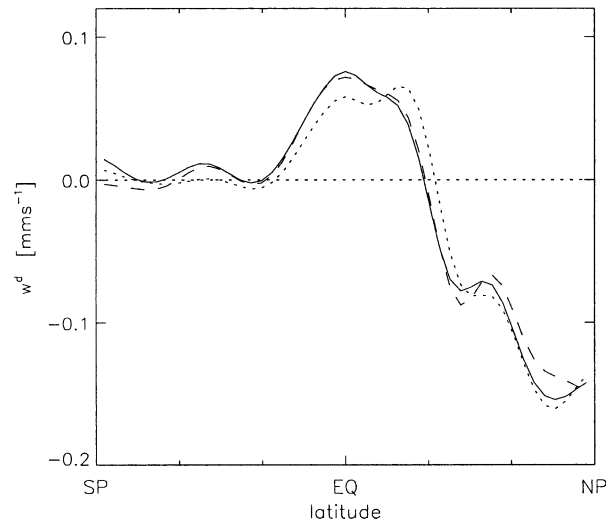


FIG. 6. Diabatic vertical velocity w^d from the zonally symmetric model forced with the EP flux divergence output from the seasonally varying wave-one model integration Z_{seasonal} (solid), along with the corresponding w^d from the wave-one model integration W_{seasonal} (dashed), both annually averaged over the 10th yr of simulation. Also shown dotted is the steady-state w^d from Z_{mean} obtained with thermal and momentum forcing equal to the annual average of that used in Z_{seasonal} .

agreement is obtained despite the spatial and temporal smoothing of the zonal force, consistent with the expectation that it is the broad-scale structure of the zonal force that is important in determining the response. In particular, note that the zonally symmetric model accurately reproduces the broad region of upwelling throughout the Tropics and well into the opposite hemisphere.

Figure 6 also shows the response to Z_{mean} (dotted line), the steady-state calculation forced with the time-averaged values of the thermal and momentum forcing used

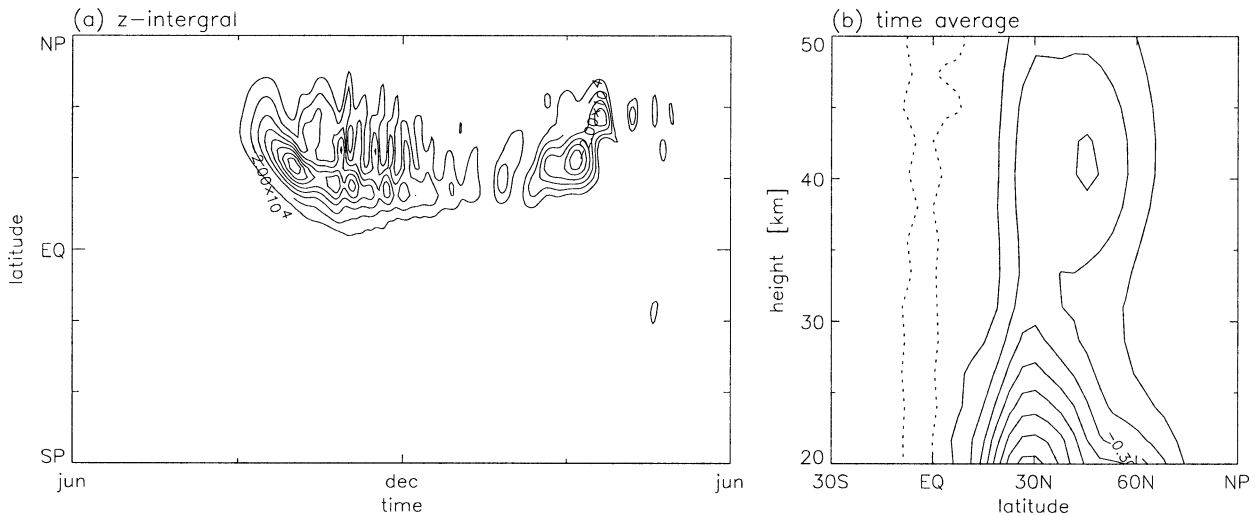


FIG. 5. The EP flux divergence from W_{seasonal} used to force the zonal model integration Z_{seasonal} : (a) vertically integrated from $z = 20$ to the upper boundary and (b) the annual average. Units: (a) $2\pi a^3 \rho_s \times 10^{-7} \text{ m}^2 \text{ s}^{-2}$ and (b) as in Fig. 2.

in Z_{seasonal} . The tropical upwelling in the seasonally varying Z_{seasonal} is about 25% greater than that in the steady Z_{mean} , which is an increase similar to that found by PE99, although for different reasons, to be discussed presently. Larger increases (up to around 50%) have also been obtained in the same model used here by different choices of radiative basic states.

The seasonally varying radiative equilibrium temperature used by PE99 (their T_e) had a kink at the equator and nonzero latitudinal gradient arbitrarily close on the winter side. Considering as an example the linearized TEM equations, the singular curvature of the annually averaged T_e at the equator gives rise to a two-cell Hadley circulation with significant upwelling in the Tropics. As pointed out by PE99, the increase in tropical upwelling obtained by including this seasonal cycle in heating is essentially due to the linear superposition of the wave-driven circulation and the Hadley circulation.

In the present case, however, the radiative equilibrium (potential) temperature θ_R has no gradient at the equator, resulting in a much smaller thermally driven circulation, as described in section 3b above. Thus, the increase seen in Fig. 6 cannot be accounted for by a linear superposition of the wave-driven and thermal circulations. We postulate instead that the seasonal cycle in thermal forcing alters the instantaneous angular momentum distribution in such a way that the downward control influence of the zonal momentum forcing can be felt closer to the equator. This can happen when the tilting of the angular momentum contours is temporally in phase with the zonal momentum forcing, leading to a nonzero time

average for the term J appearing in (1). This mechanism is discussed in more detail in sections 4b and 5b.

Observations of the lowermost stratosphere indicate that the maximum values of tropical upwelling are located in the summer hemisphere, and that the total region over which upwelling occurs also shows a seasonal migration toward the summer hemisphere (Rosenlof 1995; PE99). In the present model the wave forcing is confined to the NH winter, so most of the annual average w^d comes from the NH winter response to forcing. Thus a maximum w^d in the summer hemisphere would appear in the annual average of Fig. 6 as a maximum in the SH. It is seen from Fig. 6 that the addition of the seasonal cycle (difference between solid and dotted lines) alters the structure of w^d so that its maximum lies over the equator rather than at 25°N. Thus, although the structure of w^d obtained with the seasonal cycle does not have a maximum in the SH, the change induced by the addition of the seasonal cycle is such as to bring the structure of w^d closer to that suggested by observations.

b. Compact zonal forcing

To isolate the relation between the zonal momentum forcing and the induced low-latitude upwelling, we consider a simplification of the form of the forcing distribution. In this section the force has a compact form with a maximum of $A(t)$ at a variable latitude ϕ_0 and fixed altitude $z = 40$ km, decaying smoothly to zero within 15° on either side of the maximum, and within 20 km above and below:

$$F = \begin{cases} A(t) \cos^2\left(\frac{\pi|\phi - \phi_0|}{2 \cdot 15^\circ}\right) \cos^2\left(\frac{\pi|z - 40 \text{ km}|}{2 \cdot 20 \text{ km}}\right), & |\phi - \phi_0| \leq 15^\circ, \quad |z - 40 \text{ km}| \leq 20 \text{ km} \\ 0, & \text{otherwise.} \end{cases} \quad (7)$$

We first consider the steadily forced case $A(t) = A_0 \equiv -10^{-5} \text{ m s}^{-2} \approx -1 \text{ m s}^{-1} \text{ day}^{-1}$, which is a physically reasonable value in terms of the magnitude of the response produced. The forcing amplitude is reduced by a factor of 100 [i.e., setting $A(t) = A_0/100$] in some of the experiments below to investigate the linear dependence of the model response. The radiative relaxation rate is fixed at $\alpha = 0.05 \text{ day}^{-1}$ throughout the model domain. The vertical viscosity is set to zero to allow an easier consideration of the effect of the horizontal hyperdiffusion below. All the experiments in the remainder of this section are run at the higher resolution of $M = 64$ latitudinal modes.

1) RESTING ATMOSPHERE

We first consider the case where the radiative equilibrium potential temperature corresponds to a resting

atmosphere; that is, θ_R is constant throughout the model domain and is constant in time (no seasonal cycle).

Figure 7a shows w^d at 17 km for four different latitudinal locations of the imposed momentum forcing, given by (7) with $\phi_0 = 40^\circ, 30^\circ, 25^\circ,$ and 20° . Each simulation was run for 2000 days, which was found to be long enough to reach a sufficiently steady state. The curves are ordered with the maxima and minima in w^d occurring further poleward for larger ϕ_0 . For $\phi_0 = 40^\circ$ the response lies entirely in the NH extratropics, with upwelling on the equatorward flank of the forcing region and downwelling on the poleward flank. The slight latitudinal spread of the response beyond the latitudinal extent of the forcing is a result of the model diffusion, here a scale selective ∇^8 hyperdiffusion acting in the horizontal. This effect is discussed in more detail in section 5a.

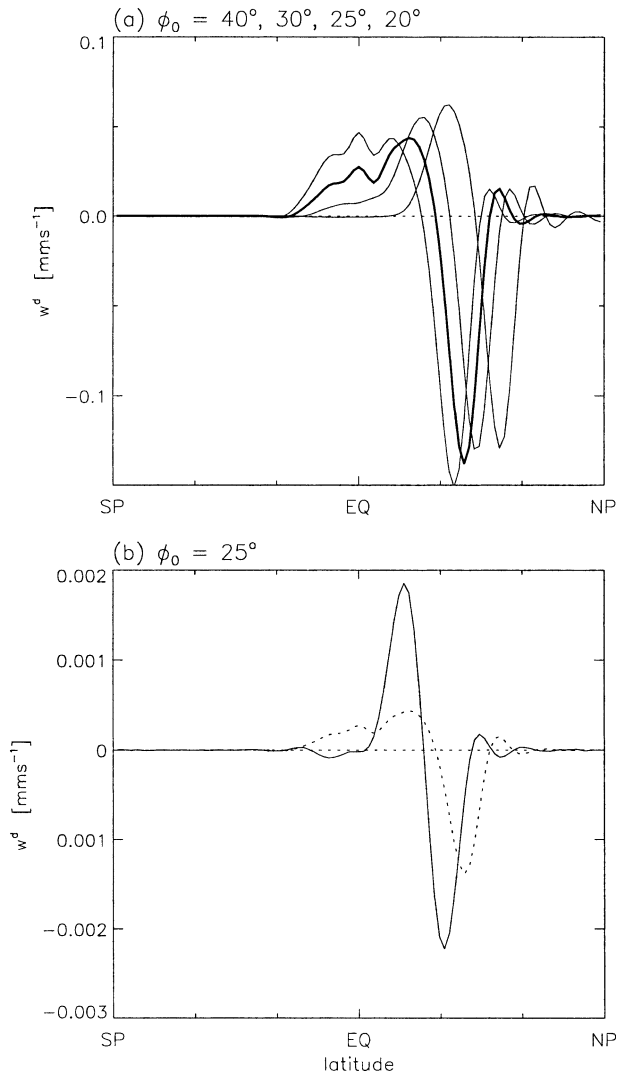


FIG. 7. Diabatic vertical velocity w^d at 17 km from the zonally symmetric model forced with the compact zonal momentum force of (7): (a) with forcing amplitude $A = A_0$ and (with peaks moving equatorward) $\phi_0 = 40^\circ$, $\phi_0 = 30^\circ$, $\phi_0 = 25^\circ$ (heavy), $\phi_0 = 20^\circ$; (b) for $\phi_0 = 25^\circ$ with $A = A_0/100$ (solid) and $A = A_0$ (dotted and rescaled by a factor of 1/100). Values are calculated after 2000 days of simulation except the solid line in (b), which is calculated after 20 000 days and has also had the thermal response removed.

As ϕ_0 is decreased the response increasingly spreads across the Tropics and into the opposite hemisphere. The dependence of the upwelling in the Tropics is different from that of the downwelling in midlatitudes. Whereas in midlatitudes the response simply shifts to lower latitudes with decreasing ϕ_0 , in low latitudes there is a systematic increase in the upwelling throughout the Tropics. For $\phi_0 = 25^\circ$ (heavy line), there is a distinct subtropical upwelling maximum, presumably a direct response to the forcing overhead, and a weaker, but substantial, broad region of upwelling extending across the Tropics and into the opposite hemisphere. For forcing at still lower latitudes, $\phi_0 = 20^\circ$, these two regions

begin to merge into a single upwelling maximum centered over the equator. In the remainder of this paper we will focus on the case $\phi_0 = 25^\circ$, and look more closely at the nature of the tropical upwelling response.

The momentum forcing in the case $\phi_0 = 25^\circ$ is zero equatorward of 10°N . Assuming linearity, that is, that the angular momentum distribution of the basic state remains unaltered by the forcing, the downward control integral of (1), predicts an upwelling response that is also zero equatorward of 10°N , since the angular momentum contours, in this case of a resting atmosphere, are vertical. Therefore, the broad region of tropical upwelling seen in Fig. 7a, must either result from additional zonal forces arising from the effects of model diffusion (PE99) or else there must be significant departures from linearity.

Considering $\phi_0 = 25^\circ$, Fig. 7b shows the response to forcing amplitude $A(t) = A_0/100$ (solid line), one-hundredth of the value used in Fig. 7a (the response to which is reproduced, scaled appropriately, in Fig. 7b as the dotted line). For this small amplitude $A = A_0/100$ of mechanical forcing, the response to thermal forcing alone is comparable to the response to mechanical forcing, and so the response to thermal forcing is subtracted out to enable comparison of the $A = A_0/100$ and $A = A_0$ responses.¹ Comparison of the two responses reveals two effects. First, in midlatitudes and in the subtropics the response for $A = A_0$ appears to be shifted poleward and reduced in magnitude. In particular, the response does not scale linearly as the forcing is increased from $A = A_0/100$ to $A = A_0$. Second, upwelling throughout the Tropics and into the opposite hemisphere is only obtained for $A = A_0$; the case $A = A_0/100$ shows a distribution closer to that which would be obtained from (1) applied to a resting atmosphere. Therefore, if model diffusion is indeed responsible for the tropical upwelling obtained with $A = A_0$, it appears that the precise way in which it acts is still fundamentally nonlinear.

An idea of the degree of nonlinearity in the above case, $\phi_0 = 25^\circ$, can be obtained by considering the distribution of angular momentum m of the steady-state responses for $A = A_0/100$ and $A = A_0$ (Figs. 8a,b). The difference between the two responses in midlatitudes seen in Fig. 7b arises from the bunching together of m contours in the region of the forcing in the case $A = A_0$. This bunching together increases the local gradient m_ϕ , resulting in a reduction of the induced circulation from (1). The tilt induced in the m contours by the forcing is also responsible for the poleward shift in the downwelling branch of the circulation around 40°N .

In low latitudes, the effect of the strong forcing on the m distribution creates a broad region of weak m gradients in the upper stratosphere, which intrudes into the forcing region at 15°N and 40–50-km altitude. Thus

¹ The smallness of the circulation in the case with $A = A_0/100$ means that the dynamics is essentially linear (except possibly very close to the equator) and so this subtraction is justified.

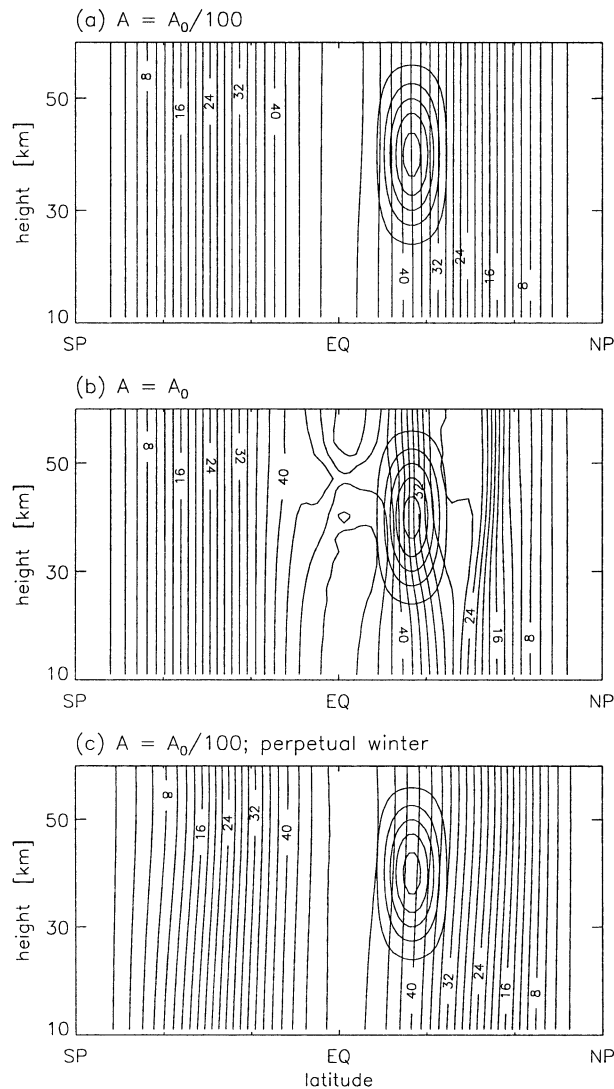


FIG. 8. Angular momentum distribution for the calculations illustrated in Figs. 7b and 9. (a) Thermal forcing corresponding to a resting atmosphere and momentum forcing amplitude $A = A_0/100$, (b) thermal forcing corresponding to a resting atmosphere and momentum forcing amplitude $A = A_0$, and (c) thermal forcing corresponding to winter solstice conditions and momentum forcing amplitude $A = A_0/100$. Units: $6.4 \times 10^7 \text{ m}^2 \text{ s}^{-1}$. The closed contours represent the momentum forcing with contour values 0.1, 0.3, . . . , 0.9 of the maximum amplitude.

the low-latitude forcing is able to drive a circulation that connects across the equator and into the opposite hemisphere, relying only on the distortion of the basic state m distribution by the forcing itself. In the case of weak forcing $A = A_0/100$ (Fig. 8a) the distortion of the tropical distribution of m is correspondingly weak and no cross equator circulation is possible.

2) PERPETUAL WINTER

Another way in which the distribution of m can be altered is by the action of the seasonal cycle in radiative

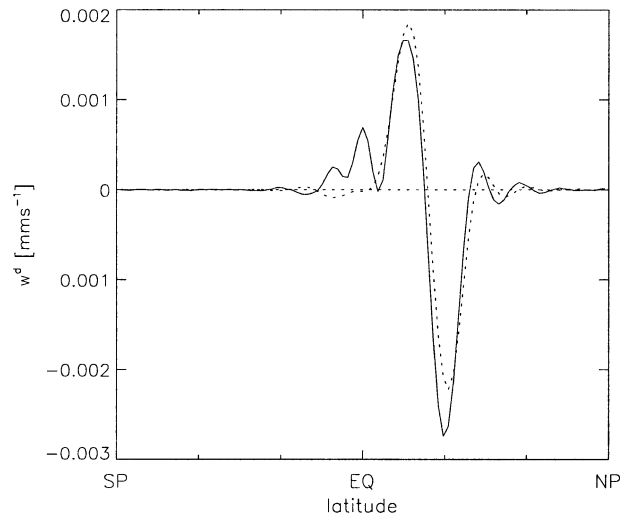


FIG. 9. Diabatic vertical velocity w^d at 17 km with forcing amplitude $A = A_0/100$, $\phi_0 = 25^\circ$, and steady radiative basic state corresponding to perpetual winter (solid) and a resting atmosphere (dotted).

heating. For example, in winter the strong westerlies in midlatitudes result in m contours that tilt poleward with height in the middle stratosphere, as shown in Fig. 8c. As can be seen from (1), zonal forcing at a given height and latitude will then result in an upwelling response that extends downward and equatorward of the latitude of the forcing (see also Haynes et al. 1991, their Fig. 8). If the zonal forcing is located in sufficiently low latitudes, this tilting of the upwelling response by the distribution of m may bring the response close to the region of weak m gradients at the equator where unforced latitudinal motion is possible, resulting in upwelling throughout the Tropics. The role of this mechanism in the upper stratosphere has also been considered recently by Tung and Kinnersley (2001).

The distribution shown in Fig. 8c was obtained using thermal forcing equal to solstice conditions of the seasonal cycle described in the following section. The zonal momentum forcing was as above, given by (7) with $A = A_0/100$ to avoid the nonlinear redistribution of m , and with $\phi_0 = 25^\circ$. Figure 9 shows the response w^d to these forcings (solid line). Because of the tilt in the m contours associated with the radiative equilibrium temperature distribution, the low latitude zonal forcing is again able to induce a cross-equator circulation resulting in mean upwelling into the opposite hemisphere. Here, however, the effect is a linear one since the weak forcing does not induce a noticeable change in the distribution of m . For comparison, the dotted line in Fig. 9 shows the response to the same momentum forcing in a resting atmosphere.

3) SEASONAL CYCLE

In sections 3 and 4a it was shown that the low-latitude upwelling obtained with time-varying thermal and mo-

mentum forcing was greater than that obtained with constant thermal and momentum forcing equal to the time average of the time-varying forcing. We now use the compact forcing profile given by (7) to investigate in more detail how the seasonal cycle influences the response. The radiative equilibrium temperature has been modified from that used in section 3 to be antisymmetric about the equator, so that the time average basic state corresponds simply to a resting atmosphere.² The momentum forcing is given by (7) with $\phi_0 = 25^\circ$ and with a seasonal cycle in $A(t)$ defined by

$$A(t) = \begin{cases} \frac{A_0}{2} \left(1 - \cos \frac{2\pi(t - 60 \text{ days})}{240 \text{ days}} \right), & |t - 180 \text{ days}| \leq 120 \text{ days} \\ 0, & \text{otherwise,} \end{cases} \quad (8)$$

giving a maximum forcing in midwinter on day 180, and zero forcing during the summer, days 0–60 and 300–360 (where, for simplicity, 1 year = 360 days). The annually averaged amplitude $\langle A(t) \rangle = 1/3A_0$, where as before $A_0 \equiv -1 \times 10^{-5} \text{ m s}^{-2}$.

Figure 10 shows the annually averaged response to seasonally varying thermal and momentum forcing (solid) and the steady-state response to steady forcing equal to the annually averaged thermal and momentum forcing (dotted). As for the steady-state calculations described above there is a marked difference between the strongly forced [with amplitude $A(t)$ as given by (8)] and the weakly forced [with amplitude $A(t)/100$] cases, shown in Figs. 10a and 10b, respectively. Again, we attribute these differences to the nonlinear adjustment of m to the strong forcing, both in midlatitudes and in the Tropics.

In both the strongly and weakly forced cases there is also an equatorward shift in the w^d response and significant increase in the tropical upwelling when the seasonal cycle is included. This can be understood by consideration of the perpetual winter case above, which showed a distortion of the m contours by the radiative forcing that allowed the effect of the zonal momentum forcing to be felt at lower latitudes. In the seasonally varying cases here, the distortion of m by the radiative forcing is in phase with the zonal momentum forcing, resulting in a bias of the upwelling toward lower latitudes. This effect appears in (1) through the term J , since the annual average and steady-state angular momentum distributions are approximately equal, by construction. With strong zonal momentum forcing J is fully nonlinear since changes in m arise in response to the forcing. On the other hand, for weak zonal momentum

² For reference, the coefficients detailed in Scott and Haynes (2002), Eq. (6) have been changed to $u_0 = 30$, $u_1 = -u_2 = 150$, $b_0 = 0.01$, $b_1 = b_2 = 0.06$, $\phi_0 = 0$, $\phi_1 = -\phi_2 = 60$, $a_1 = a_2 = 0.04$, and $z_1 = z_2 = 55$. The zonal mean zonal velocity basic state determined by these coefficients is similar to that shown in Scott and Haynes (2002), Fig. 2.

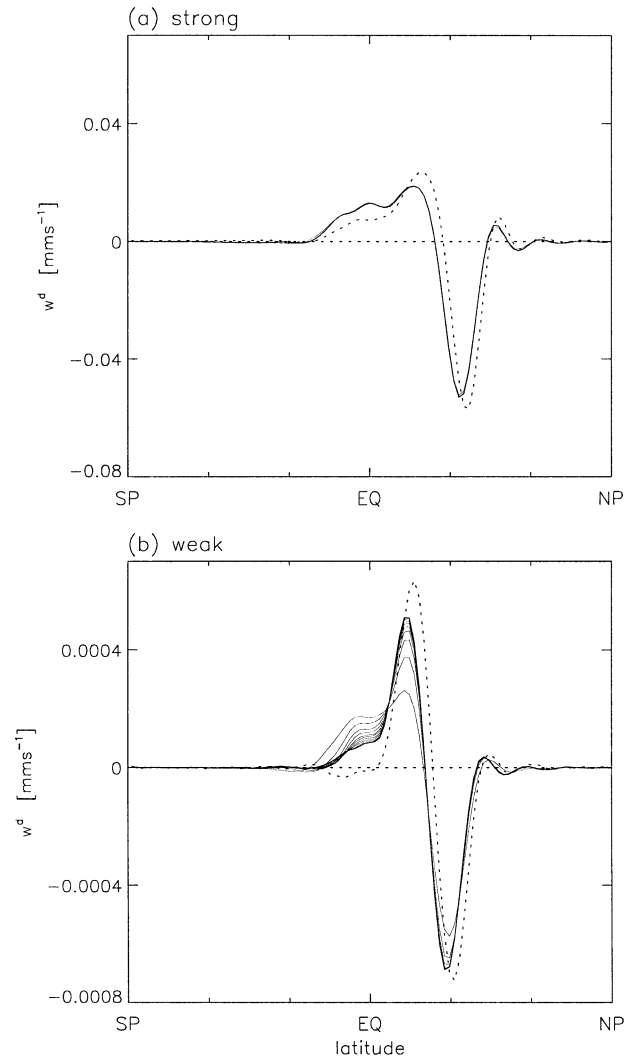


FIG. 10. Annual average of the seasonally varying response (solid) and the corresponding steady-state response (dotted): (a) strong forcing, $A(t)$ given by (8) (solid) and $A(t)$ given by the annual average of (8) [i.e., $A(t) = \langle A(t) \rangle = 1/3A_0$] (dotted); (b) weak forcing, with forcing amplitude 1/100 that used in (a). The light solid lines denote the annual average values at 5-yr intervals for the cases with a seasonal cycle, w^d decreasing in magnitude at the equator with increasing time.

forcing J is linear, since the changes in m are imposed externally by the radiative heating. Thus, the difference between the solid and dotted lines in Fig. 10b can be explained by J , even though the forcing is so weak that the dynamics are essentially linear. Note, the convergence to a constant time-averaged upwelling in the weakly forced seasonally varying case, Fig. 10b, is very slow, the thin lines denoting the annual averages every 5 yr (1800 days).

5. Discussion

The results presented above indicate that nonlinearity in the steady-state case and transience in the seasonally

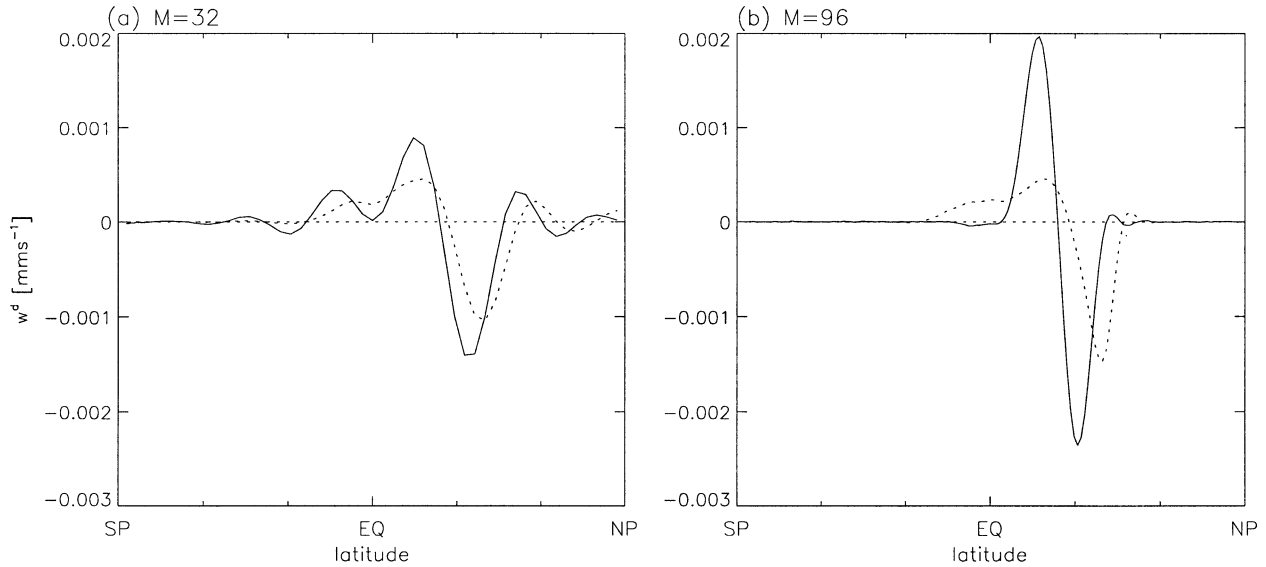


FIG. 11. As in Fig. 7b, except with a model resolution of: (a) $M = 32$ meridional modes and (b) $M = 96$ meridional modes. The solid and dotted lines represent the responses to momentum forcing with amplitude $A(t) = A_0/100$ and $A(t) = A_0$, respectively, with the response for $A(t) = A_0$ rescaled by a factor of $1/100$.

varying case can both alter the distribution of angular momentum so that a zonal momentum force in low latitudes can induce an upwelling circulation across the Tropics and into the opposite hemisphere. In this section we consider these effects in more detail and some of their implications for the wave-one calculations presented in section 3.

a. Hyperdiffusion

For stability, the model used in all the above experiments contains a scale selective ∇^8 hyperdiffusion that acts on the momentum equation. As discussed by PE99 such artificial diffusion can contribute to a tropical circulation, since the zonal force required to balance latitudinal motion is small close to the equator. Although PE99 considered vertical viscosity similar arguments apply to horizontal diffusion of the kind used here. There is no explicit vertical viscosity in the model equations used here.

To see how the latitudinal scale of the induced circulation depends on the hyperdiffusion, we consider the following simple scaling arguments. Using similar analysis to that used in Holton et al. (1995) and Garcia (1987) the linearized TEM equations on the sphere (e.g., Holton et al. 1995), with a frictional force $-\kappa u$ in the zonal momentum equation, lead to a steady-state relation of the form

$$\begin{aligned} \frac{\partial}{\partial z} \left[\frac{1}{\rho_0} \frac{\partial}{\partial z} (\rho_0 w) \right] + \frac{\kappa}{\alpha} \frac{N^2}{4\Omega^2 a^2 \cos\phi} \frac{\partial}{\partial \phi} \left(\frac{\cos\phi}{\sin^2\phi} \frac{\partial w}{\partial \phi} \right) \\ = \frac{1}{2\Omega a \cos\phi} \frac{\partial}{\partial \phi} \left(\frac{\cos\phi}{\sin\phi} \frac{\partial F}{\partial z} \right), \end{aligned} \quad (9)$$

where κ is the friction timescale, α is the radiative timescale, and other variables are as in Holton et al. (1995). If the frictional term is replaced by a hyperdiffusion of the form $-\kappa' \nabla^8 u$ (as in our model), then κ in (9) can be replaced by a term of order $\gamma_{\max} \delta^8 / L^8$, where γ_{\max} is the rate at which the smallest wavenumbers are damped, δ is their length scale (i.e., the grid resolution), and L is a horizontal length scale. Balancing terms of (9) outside the forcing region, that is, where $F = 0$, leads to the following scaling for L :

$$L \sim \left(\frac{\gamma_{\max}}{\alpha} \right)^{1/10} \delta^{4/5} \left(\frac{ND_-}{\Omega} \right)^{1/5}, \quad (10)$$

in midlatitudes ($a \sin\phi \sim a/2$) and

$$L \sim \left(\frac{\gamma_{\max}}{\alpha} \right)^{1/12} \delta^{2/3} \left(\frac{aND_-}{2\Omega} \right)^{1/6}, \quad (11)$$

in low latitudes ($a \sin\phi \sim L$), where $D_- = \sqrt{\min(HD, D^2)}$, with a vertical length scale D , and a vertical scale height $H = 7$ km. In (10) and (11), L is the scale on which an upwelling response decays away from the forcing region. Note that L depends very weakly on γ_{\max} , so that moderate changes in the hyperdiffusion will have little effect on L , but depends more strongly on the resolution δ . For example, in the Tropics, resolutions of $M = 32, 64,$ and 96 meridional modes give $L \approx 1200, 750,$ and 580 km, respectively. In midlatitudes $M = 64$ gives $L \approx 570$ km.

Figures 11a and 11b show the dependence of the response on the resolution for steady forcing with $A = A_0/100$ (solid) and $A = A_0$ (dotted). These should be compared with Fig. 7b. For both strong and weak forcing, higher resolution gives a tighter response in mid-

latitudes, approximately following the above scaling. However, the low-latitude response to strong forcing (dotted lines) is unaffected by the resolution, which supports the assertion made in section 4b that the low-latitude response is nonlinear for $A = A_0$.

Since the diffusion acts to spread the response latitudinally away from the forcing region, its presence will increase the effect described in section 4b above, namely, that the tilting of angular momentum contours can lead to increased tropical upwelling. For even if the tilting m contours fail to link the forcing region with the region of weak m gradients in the Tropics, the latitudinal spreading of the circulation by the diffusion may be sufficient to bridge the gap. As an example, if the seasonal cycle in thermal heating induces a tilt in the m contours (see Fig. 8c) of around 5° between the forcing region (maximum at 40 km) and where the upwelling is measured (here at 17 km), and if we take the latitudinal spreading of the response in the Tropics with $M = 64$, that is $750 \text{ km} \sim 7.5^\circ$, then forcing at 12.5°N will penetrate to the region of weak m gradients at the equator. In weakly forced cases of Figs. 9 and 10b, the forcing is nonzero north of 10°N and so a small circulation is able to penetrate through the Tropics.

b. The effect of the transient term

As we saw in section 4b, the addition of a seasonal cycle in thermal and mechanical forcing can influence the tropical upwelling response, even in the almost linear regime with very weak momentum forcing. One way in which this can happen is through the transient interaction of the momentum forcing and the distribution of m : the momentum forcing occurs predominantly during winter, at the same time as the thermal forcing induces a poleward and upward tilt in the m contours. The transient interaction is represented in (1) by the term J defined by

$$J = \psi'_\phi m'_z - \psi'_z m'_\phi \quad (12)$$

$$= -\rho_0 \cos\phi (aw'm'_z + v'm'_\phi), \quad (13)$$

where the primes denote deviations from the time average. In general, the second term on the right-hand side, $v'm'_\phi$, is much larger than the first, and so J represents the horizontal advection of m . As mentioned above, J can be nonzero even for weak forcing, since the transience in m_ϕ arises from the thermal forcing independently of the amplitude of the momentum forcing. For strong forcing on the other hand, $\mathcal{O}(1)$ transience in both v and m_ϕ can also arise as a result of the transience in the momentum forcing itself.

In model simulations it was found that the biggest changes to the steady-state circulation were usually obtained when both the thermal and mechanical forcing were made time varying. This suggests that the role of the seasonal variations in thermal forcing cannot be neglected. The effect of the transience in the momentum

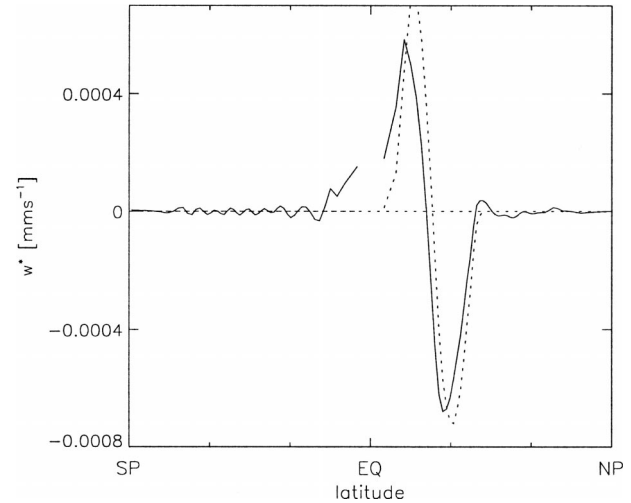


FIG. 12. Vertical velocity at 17 km calculated from (1) with $A(t)$ given by (8) with $\phi_0 = 25^\circ$ and $A = A_0/300$, and with J taken from the corresponding calculation with seasonal cycle $[A(t)$ given by (8) divided by 100] shown in Fig. 10b (solid). The dotted line is the same but without the term J .

forcing may be most significant at very low latitudes, where a zonal force is balanced preferentially by a zonal acceleration rather than by a Coriolis torque due to a meridional circulation.

To isolate the response to the above transient interaction from the effects of model diffusion, consider w given by (1), where J has been evaluated using the model fields output from the weakly forced seasonal calculation described in section 4c [$A(t)$ given by (8) divided by 100]. The response w , shown in Fig. 12 (solid line), was obtained by interpolating F , J , etc., onto a regular grid in (m, z) space to obtain $F(m, z)$, etc., performing the integral and derivative, and plotting the result against $\phi(m, z)$ at $z = 17 \text{ km}$. Also shown (dotted line) is the same calculation but leaving out the term J . Although the calculation does not allow the evaluation of w very close to the equator, one nevertheless sees a clear increase in the tropical upwelling when the term J is included. Further, the increase seen here is in rough agreement with the increase seen between the solid and dotted lines in Fig. 10b, the seasonal cycle and steady-state responses, respectively. Note that the small differences between Figs. 12 and 10b arise from the neglect of unresolved diffusive forces in the integrand of (1), that is, the neglect of the hyperdiffusive effects discussed in section 5a.

c. The zonally asymmetric response and the observed circulation

The effective momentum forcing on the zonal flow in the wave-one experiments of section 3, namely, the EP flux divergence, was closer to the strong forcing amplitudes used in section 4 than to the weak forcing amplitudes. As seen in Fig. 2, the distribution of m in

low latitudes is significantly distorted from the vertical, similar to the zonally symmetric case shown in Fig. 8b. The region of weak m gradients is larger for the stronger EP flux divergence of $h_0 = 270$ m. In both cases $h_0 = 240$ and $h_0 = 270$ the EP flux divergence extends toward the edge of the region of weak m gradients but not far enough into it to account for the penetration of the tropical upwelling well into the opposite hemisphere. In the light of the analysis in section 5a, it seems reasonable that the model diffusion is acting here to spread the response of the wave forcing latitudinally to the extent where it can drive a significant circulation through the region of weak m gradients in the Tropics. The length scale for the latitudinal spreading by diffusion in this case is around 12° .

In section 4, the compact forcing centered on $\phi_0 = 25^\circ\text{N}$ extended to 10°N , and the m contours in the perpetual winter case allowed a penetration of the circulation into the Tropics (Fig. 8c). In the stratosphere, the edge of the surf zone lies near 20°N , in approximate agreement with the edge of the EP flux divergence in Fig. 2. Thus, the distribution of m needs to be relatively strongly distorted to provide a link between the wave forcing region and the Tropics. Although thermal heating alone may be insufficient to cause such a strong distortion, it may combine with the additional nonlinear distortion of m by the momentum forcing (e.g., Figs. 2 and 8b) to create this link into the Tropics.

Finally, we note that in none of the above experiments was an upwelling maximum produced in the opposite hemisphere to the forcing. Although the addition of such features as the seasonal cycle, model diffusion, and nonlinearity all contribute to an increase in the tropical upwelling, and an apparent shift of the response to lower latitudes, it is possible that these are nevertheless unable to produce such a maximum. A more plausible explanation for this feature of the observed circulation may be simply the presence of summer hemisphere wave drag.

6. Conclusions

We have used a simple mechanistic model of the stratosphere to investigate the mean meridional circulation response of an atmosphere subjected to zonal momentum and radiative forcing, with particular emphasis on the low-latitude tropical upwelling. Both a zonal wavenumber-one model, in which zonal momentum forcing arose self-consistently from wave dissipation, and a zonally symmetric model, in which the momentum forcing was derived from the wave-one model, produced circulations that are in good agreement with each other and with the vertical velocities derived from observations of the real stratosphere. Further experiments using the zonally symmetric model with compact momentum forcing investigated in more detail the importance of nonlinearity, model diffusion, and the transient effects of the seasonal cycle.

As discussed in a recent investigation by PE99, model diffusion plays an important role in the penetration of the steady-state-induced circulation into low latitudes. In our zonally symmetric model, significant tropical upwelling can occur in the steady state if the momentum forcing extends into the subtropics, but only if the forcing is strong enough to alter the distribution of angular momentum in the Tropics. In our wave-one model with realistic wave evolution, the substantial upwelling seen throughout the Tropics can be explained by the substantial wave dissipation occurring well into the subtropics, together with effects of the model diffusion and the nonlinear adjustment of angular momentum.

The role of nonlinearity in allowing a steady-state tropical upwelling was supported by calculations in which the forcing strength was reduced significantly, as well as by calculations at different resolutions. The latter calculations showed that the tropical upwelling obtained with strong forcing was independent of the resolution (the dotted lines in Figs. 7b and 11a,b), contrary to the predictions of the linear scaling arguments in section 5b.

Modification of the annually averaged induced circulation from the steady state was found when a seasonal cycle was included in both the radiative basic state (i.e., the thermal forcing) and in the momentum forcing. In the wave-one model, the seasonal cycle in wave dissipation arose naturally from the dependence of wave propagation on the seasonally evolving basic state, whereas in the zonally symmetric model it was imposed externally. In both models the addition of the seasonal cycle resulted in an increase in the tropical upwelling. This increase was found in the zonally symmetric model even when the zonal momentum forcing was weak, so that the dynamics were approximately linear (Fig. 10). Thus, the increase appears to arise largely from the interaction of the seasonal cycle in thermal and momentum forcing, and not from the nonlinear effect of the redistribution of angular momentum by the zonal momentum forcing.

In the real atmosphere, tilting of the angular momentum distribution by the seasonal cycle in the thermal forcing may be insufficient in itself to link the surf zone to the region of weak angular momentum gradients in the Tropics. However, it appears from the foregoing that it can certainly make the effects of extratropical wave drag be felt closer to the equator. Thus, it is possible that such tilting could combine with other effects, for example, the nonlinear redistribution of angular momentum by the wave drag, to allow extratropical wave drag to influence the circulation across the Tropics.

Acknowledgments. This work was begun while the author was completing his Ph.D. at the Department of Applied Mathematics and Theoretical Physics at the University of Cambridge, under the supervision of Peter Haynes, whose help and encouragement during this time, and subsequently, is gratefully acknowledged. The

author also wishes to thank Peter Haynes, Alan Plumb, and the referees for valuable suggestions and detailed comments on the first version of the paper. Financial support for this work was provided by the U.K. Natural Environmental Research Council and the U.K. Meteorological Office through a CASE studentship. The author thanks the Laboratoire d'Aérodynamique in Toulouse for support during the completion of this work, with financial support by the European Commission under Contract EVK2-1999-00015.

REFERENCES

- Andrews, D. G., J. R. Holton, and C. B. Leovy, 1987: *Middle Atmosphere Dynamics*. Academic Press, 489 pp.
- Dickinson, R. E., 1968: On the excitation and propagation of zonal winds in an atmosphere with Newtonian cooling. *J. Atmos. Sci.*, **25**, 269–279.
- , 1969: Theory of planetary wave–zonal flow interaction. *J. Atmos. Sci.*, **26**, 73–81.
- Dunkerton, T. J., 1989: Nonlinear Hadley circulation driven by asymmetric differential heating. *J. Atmos. Sci.*, **46**, 956–974.
- Garcia, R. R., 1987: On the mean meridional circulation of the middle atmosphere. *J. Atmos. Sci.*, **44**, 3599–3609.
- Haynes, P. H., and M. E. McIntyre, 1987: On the representation of Rossby wave critical layers and wave breaking in zonally truncated models. *J. Atmos. Sci.*, **44**, 2359–2382.
- , C. J. Marks, M. E. McIntyre, T. G. Shepherd, and K. P. Shine, 1991: On the “downward control” of extratropical diabatic circulations by eddy-induced mean zonal forces. *J. Atmos. Sci.*, **48**, 651–678.
- Held, I. M., and A. Y. Hou, 1980: Nonlinear axially symmetric circulations in a nearly inviscid atmosphere. *J. Atmos. Sci.*, **37**, 515–533.
- Holton, J. R., 1990: On the global exchange of mass between the stratosphere and the troposphere. *J. Atmos. Sci.*, **47**, 392–395.
- , P. H. Haynes, M. E. McIntyre, A. R. Douglass, R. B. Rood, and L. Pfister, 1995: Stratosphere–troposphere exchange. *Rev. Geophys.*, **33**, 403–439.
- Plumb, R. A., and J. Eluszkiewicz, 1999: The Brewer–Dobson circulation: Dynamics of the tropical upwelling. *J. Atmos. Sci.*, **56**, 868–890.
- Rosenlof, K. H., 1995: Seasonal cycle of the residual mean meridional circulation in the stratosphere. *J. Geophys. Res.*, **100**, 5173–5191.
- , and J. R. Holton, 1993: Estimates of the stratospheric residual circulation using the downward control principle. *J. Geophys. Res.*, **98**, 10 465–10 479.
- Saravanan, R., 1992: A mechanistic spectral primitive equation model using pressure coordinates. Model documentation, Dept. of Applied Mathematics and Theoretical Physics, University of Cambridge, 36 pp.
- Scott, R. K., and P. H. Haynes, 1998: Internal interannual variability of the extratropical stratospheric circulation: The low-latitude flywheel. *Quart. J. Roy. Meteor. Soc.*, **124**, 2149–2173.
- , and —, 2000: Internal vacillations in stratosphere-only models. *J. Atmos. Sci.*, **57**, 3233–3250.
- , and —, 2002: The seasonal cycle of planetary waves in the winter stratosphere. *J. Atmos. Sci.*, **59**, 803–822.
- Semeniuk, K., and T. G. Shepherd, 2001a: Mechanisms for tropical upwelling in the stratosphere. *J. Atmos. Sci.*, **58**, 3097–3115.
- , and —, 2001b: The middle-atmosphere Hadley circulation and equatorial inertial adjustment. *J. Atmos. Sci.*, **58**, 3077–3096.
- Shine, K. P., 1989: Sources and sinks of zonal momentum in the middle atmosphere diagnosed using the diabatic circulation. *Quart. J. Roy. Meteor. Soc.*, **115**, 265–292.
- Tung, K. K., and J. S. Kinniersley, 2001: Mechanisms by which extratropical wave forcing in the winter stratosphere induces upwelling in the summer hemisphere. *J. Geophys. Res.*, **106**, 22 781–22 791.
- WMO, 1985: Atmospheric ozone 1985. WMO Rep. 16.
- , 1999: Scientific assessment of ozone depletion 1998. WMO Rep. 44.
- Yulaeva, E., J. R. Holton, and J. M. Wallace, 1994: On the cause of the annual cycle in tropical lower-stratospheric temperatures. *J. Atmos. Sci.*, **51**, 169–174.